Available online at www.sciencedirect.com

ScienceDirect

Ceramics International 39 (2013) 9715–9720

CERAMICS INTERNATIONAL

www.elsevier.com/locate/ceramint

Short communication

Morphology-controlled synthesis of Ag_3PO_4 microcubes with enhanced visible-light-driven photocatalytic activity

Xuehua Yan, Qingxia Gao, Jieling Qin, Xiaofei Yang*, Yang Li, Hua Tang

School of Materials Science and Engineering, Jiangsu University, Zhenjiang 212013, China

Received 7 April 2013; received in revised form 11 April 2013; accepted 12 April 2013
Available online 24 April 2013

Abstract

Cubic Ag_3PO_4 microcrystals were synthesized by deposition–precipitation in the presence of ammonia. As-synthesized samples were characterized by field emission scanning electron microscopy (FE-SEM), X-ray diffraction (XRD), Raman spectroscopy and UV–visible diffuse reflectance spectroscopy (UV–vis DSR). Visible-light-driven photocatalytic performance of the obtained Ag_3PO_4 was evaluated for photocatalytic degradation of typical organic dye molecules. Compared to irregular Ag_3PO_4 materials prepared in the absence of ammonia, the prepared cubic samples exhibited a higher photocatalytic activity, suggesting the crucial role of the ammonia in the formation of cubic Ag_3PO_4 microcrystals. In addition, the specific cubic morphology of Ag_3PO_4 sample contributes substantially to its highly efficient visible light photocatalytic performance. Moreover, photocatalytic degradation experiments of the cubic Ag_3PO_4 toward different organic dye molecules rhodamine B (RhB), methyl blue (MB) and methyl orange (MO) were carried out. These results show that photo-generated active oxygen-containing superoxide radicals and photo-induced holes offer the major contribution to highly efficient visible light photocatalytic activity of Ag_3PO_4.

Keywords: Visible light photocatalysis; Ag_3PO_4; Cubic microcrystals; Organic dye; Radicals

1. Introduction

Over the past few decades, semiconductor photocatalysts have attracted much attention, in particular photocatalysts that are highly reactive under visible light have shown a broad range of applications from water disinfection, removal and degradation of organic pollutants, to water splitting [1–5]. Most recently, it has been reported by Ye and co-workers [6] that Ag_3PO_4 has extremely high photo-oxidative capabilities for O_2 generation from water splitting with a quantum efficiency of nearly 90% under visible-light irradiation. Moreover, it has shown that Ag_3PO_4 exhibits excellent visible-light-driven photocatalytic degradation efficiency toward organic dyes under visible light [7]. In comparison with several visible light photocatalysts currently known, including doped TiO_2, $BiVO_4$, and AgX (X=Cl, Br), Ag_3PO_4 has a significantly higher photocatalytic efficiency. This together with its superior photooxidative capabilities makes it a promising candidate for practical applications. However, several limitations of Ag_3PO_4 photocatalyst, including irregular morphology, poor solubility, low stability and the use of expensive silver-containing material, restrict its practical use. Its photocatalytic activity has also been proved to be closely related to its size, morphology and specific highly reactive facet.

In order to obtain high-quality Ag_3PO_4-based materials for potential applications in different fields, considerable efforts have been made over the past few years to the synthesis of visible light Ag_3PO_4 photocatalysts with well-defined morphologies including hierarchical Ag_3PO_4 porous microcubes [8], dendritic Ag_3PO_4 [9], nanosized Ag_3PO_4 [10,11], concave trisoctahedral Ag_3PO_4 microcrystals [12], Ag_3PO_4 tetrapods [13] and graphene-based composite photocatalysts [14–28]. Despite tremendous efforts, the synthesis and fabrication of highly active Ag_3PO_4 photocatalysts with well-defined cubic structure are still rare [29]. It is therefore urgent and

*Corresponding author. Tel.: +86 51188790191; fax: +86 51188791947.
E-mail address: xyang@ujs.edu.cn (X. Yang).

0272-8842/$ - see front matter © 2013 Elsevier Ltd and Techna Group S.r.l. All rights reserved.
http://dx.doi.org/10.1016/j.ceramint.2013.04.044

highly desirable to develop a facile and low-cost process for the controllable synthesis of Ag_3PO_4 materials with regular shape.

Herein, we report the fabrication of cubic Ag_3PO_4 microcrystals via a facile ion-exchange deposition–precipitation method by utilizing ammonia as the structure-directing agent and its highly efficient visible light photocatalytic performance. The employment of ammonia in the synthetic process may effectively tailor the morphology of Ag_3PO_4 crystals while the cubic characteristic of the photocatalyst favors improved visible-light-driven photocatalytic degradation of organic dye molecules. Furthermore, their structural and physicochemical properties were also investigated, which shows that there exists a low-cost and effective approach for a large-scale production of well-defined Ag_3PO_4 visible light photocatalysts for their applications in the removal of organic contaminants.

2. Experimental section

2.1. Synthesis of samples

In a typical synthesis, aqueous ammonia solution (20 mL, 0.1 M) was introduced dropwise into $AgNO_3$ aqueous solution (20 mL, 0.05 M) in a beaker, the mixture was stirred till 50 min in order to obtain a clear solution. After that aqueous Na_2HPO_4 solution (15 mL, 0.2 M) was added dropwise to the mixture, the reaction mixture was sealed and kept stirring for additional 30 min. The obtained precipitate was collected by centrifugation, washed several times with absolute ethanol and distilled water, and finally dried at 60 °C in vacuum overnight. For the synthesis of irregular Ag_3PO_4, all experiment conditions are kept constant while ammonia was not used as a reference.

2.2. Characterization

The morphologies of the as-synthesized samples were examined by field emission scanning electron microscopy (FESEM, JEOL, JSM-7001F). The phases of the obtained products were collected on a Bruker D8 Advance X-ray diffractometer (Cu Kα radiation, $\lambda = = 0.15406$ Å) in a 2θ range from 10° to 80° at room temperature. Raman experiments were performed using a DXR spectrometer using the 532 nm laser line and measurements were made in backscattering geometry. UV–visible diffuse reflectance spectra were recorded within 200–800 nm wavelength range using a Shimadzu UV2450 spectrometer.

2.3. Photocatalytic experiment

The optical system for the photocatalytic reaction consists of a 350 W Xe lamp and a cut-off filter ($\lambda > 420$ nm). Dye solutions (100 mL, 10 ppm) containing 50 mg of samples were put in a sealed glass beaker and ultrasonicated for 10 min. It was then stirred in the dark for 30 min to ensure absorption–desorption equilibrium. After visible light illumination, 4 mL of samples were taken out at regular time intervals (5 min) and separated through centrifugation (10,000 rpm, 10 min). The supernatants were analyzed by recording variations of the absorption band maximum in the UV–vis spectra by using a Lambda 25 UV/Vis spectrophotometer.

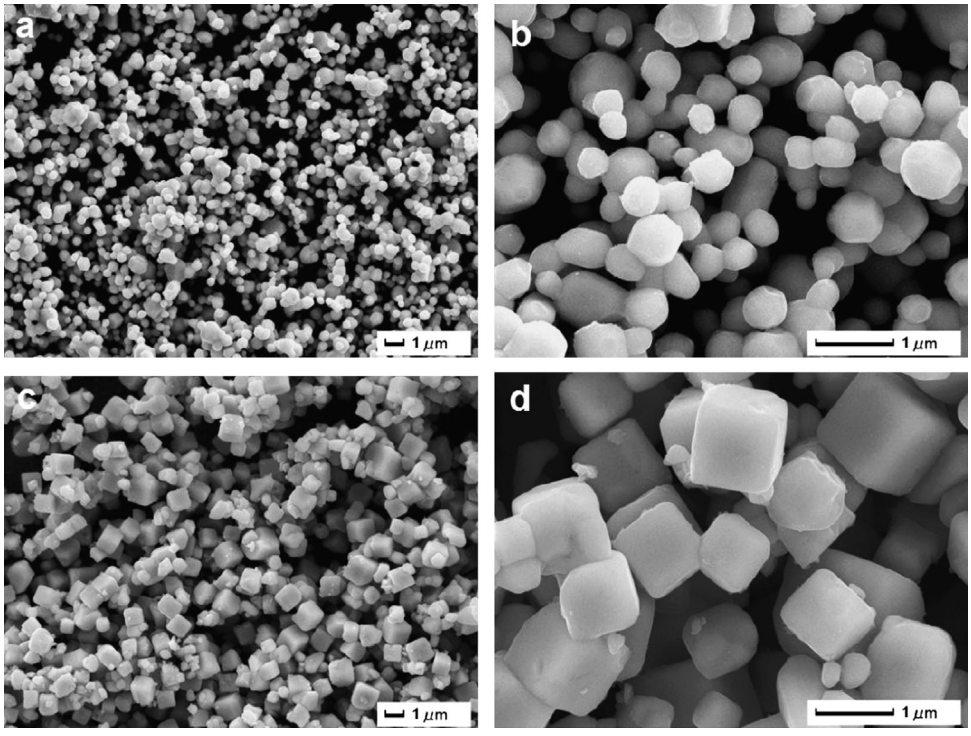

Fig. 1. Low- and high-magnification FE-SEM images of irregular (a, b), cubic (c, d) Ag_3PO_4.

3. Results and discussion

Fig. 1 shows low- and high-magnification FE-SEM images of as-prepared irregular Ag_3PO_4 and cubic Ag_3PO_4 microcrystals prepared in the absence and presence of ammonia, respectively. As shown in Fig. 1a, Ag_3PO_4 particles synthesized without using ammonia display irregular spherical-like morphologies and demonstrate good dispersibility although few aggregations were observed. Enlarged FE-SEM image reveals that the diameter of the obtained particles ranges from 0.2 μm to 0.7 μm. When the appropriate amount of ammonia was used before the addition of Na_2HPO_4 into the system, the Ag_3PO_4 microcrystals presented typical cubic morphologies while few irregular particles were also detected. In addition, high-magnification FE-SEM image confirmed the generation of cubic Ag_3PO_4 microcrystals ranging from 0.5 μm to 1 μm. In conclusion, the introduction of proper ammonia plays a vital role in obtaining relatively regular Ag_3PO_4 microcrystals with cubic structure.

In order to further investigate the effect of ammonia on the morphology of the Ag_3PO_4 samples, control experiments of the addition of Na_2HPO_4 into the mixture of $AgNO_3$ and ammonia after different stirring time (10–60 min) have been conducted and the FE-SEM images of different Ag_3PO_4 samples are shown in Fig. 2. When ammonia was added into $AgNO_3$ aqueous solution and the mixture of $AgNO_3$ and ammonia was stirred for 10 min, the subsequent introduction of Na_2HPO_4 into the above mixture caused the formation of particles with relatively uniform size while samples contained both cubic-like and irregular spherical-like particles. When the stirred time was extended to 20 min, particles become more irregular accompanying with the presence of larger cubic-like particles than those obtained at the stirring time of 10 min. Further increase of stirring time from 20 min to 30 min results in the generation of triangle-like larger particles together with irregular smaller particles. When Na_2HPO_4 was added into the mixture of $AgNO_3$ and ammonia after a stirring time of 40 min, more cubic-like particles were formed while holes

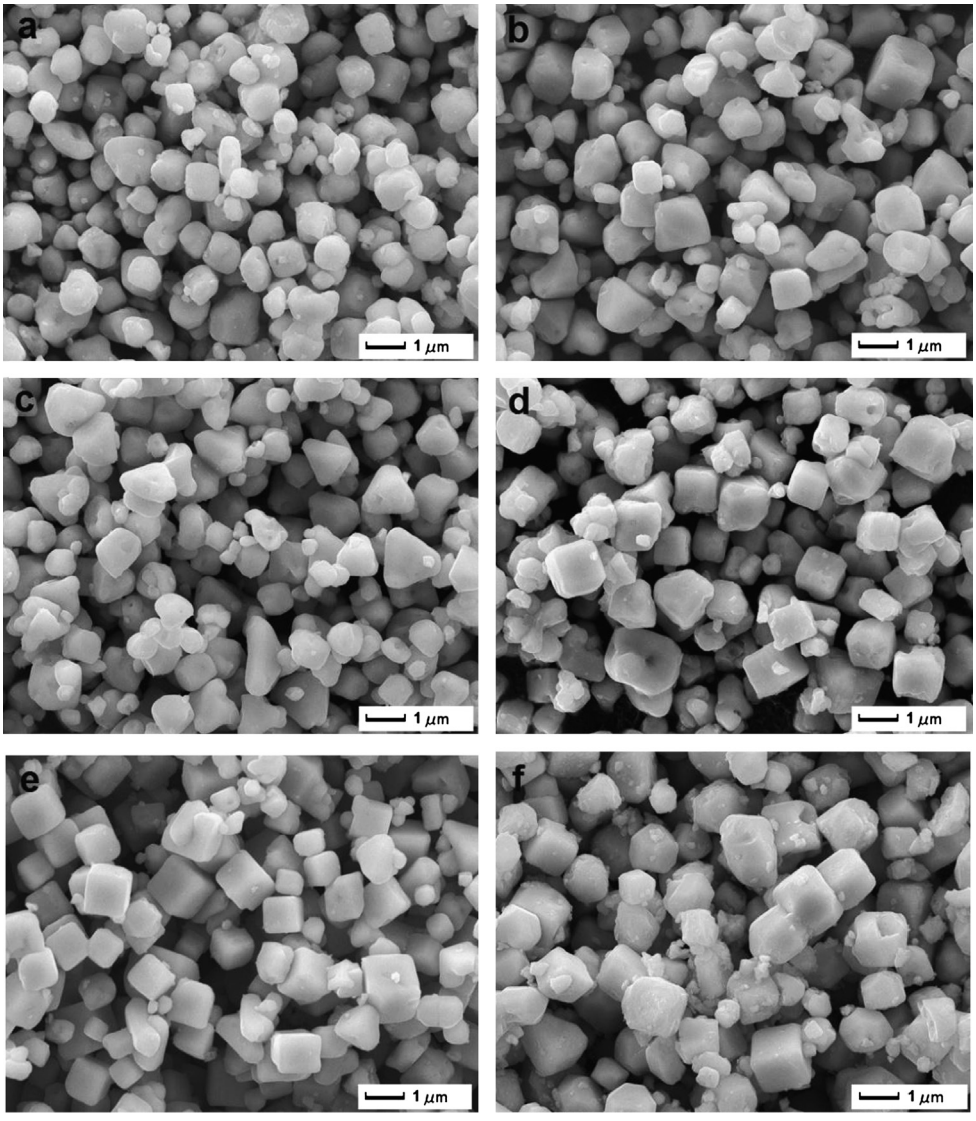

Fig. 2. FE-SEM images of as-synthesized Ag_3PO_4 samples obtained by mixing $AgNO_3$ and ammonia under different stirring time: (a) 10 min; (b) 20 min; (c) 30 min; (d) 40 min; (e) 50 min and (f) 60 min.

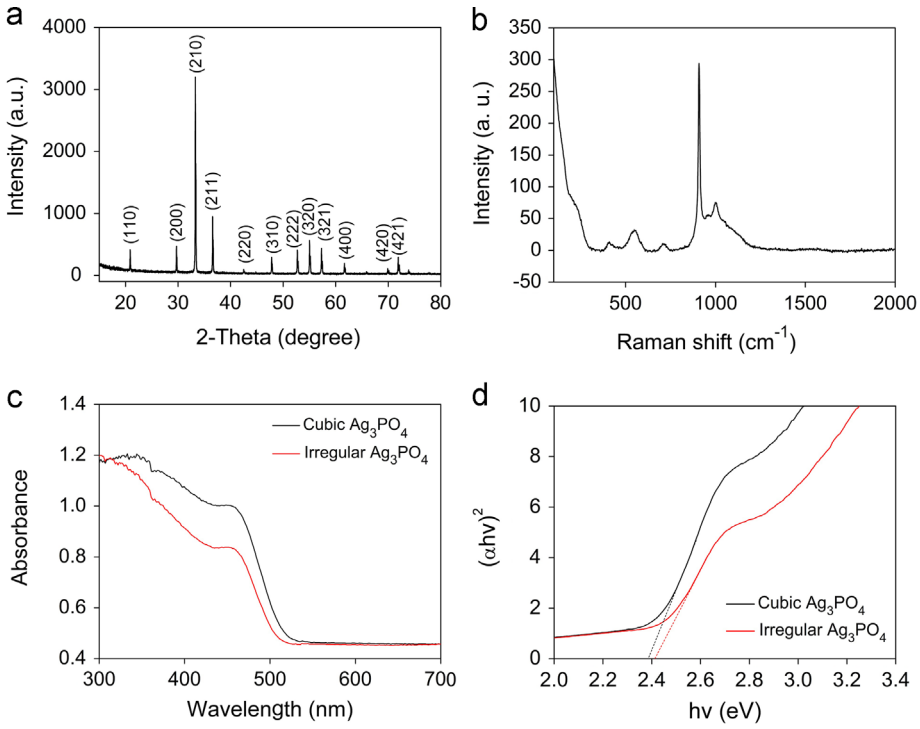

Fig. 3. XRD pattern (a) and Raman spectrum (b) of cubic Ag_3PO_4 microcrystals; UV–vis diffuse reflectance spectra (c) and the plot of $(\alpha hv)^2$ versus energy (hv) (d) of as-prepared cubic Ag_3PO_4 microcrystals and irregular Ag_3PO_4.

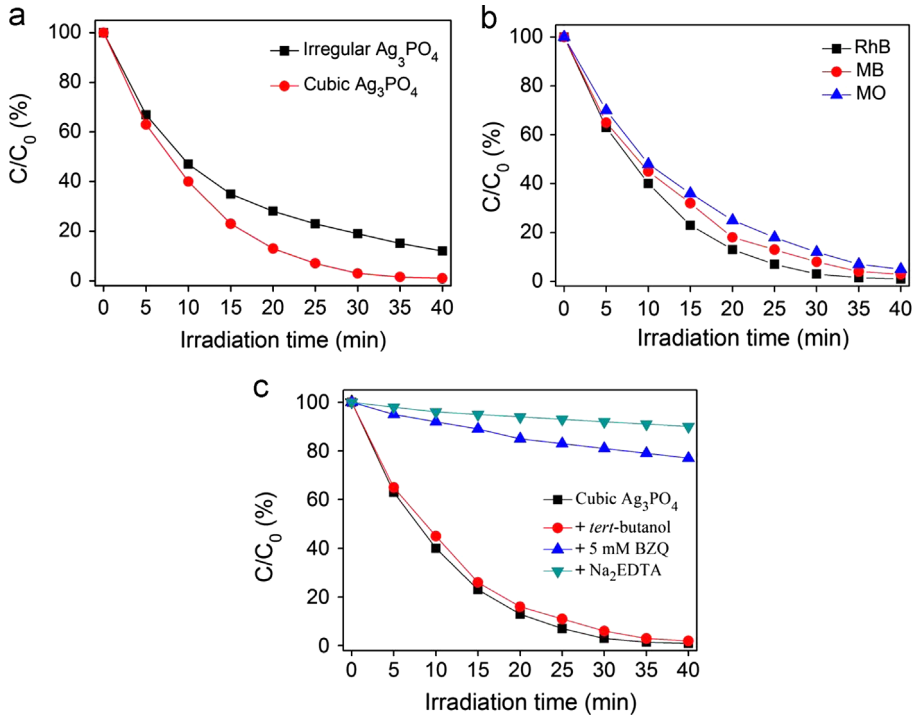

Fig. 4. (a) Photocatalytic degradation curves of cubic Ag_3PO_4 and irregular Ag_3PO_4 over RhB; (b) photocatalytic performance of cubic over different organic dyes and (c) reactive species trapping experiments of cubic Ag_3PO_4 photocatalyst over RhB.

and defects were observed on the surface. The holes and defects were found to be improved by the extension of stirring time from 40 min to 50 min while the obtained samples demonstrate typical cubic morphology with smooth surfaces. An extra stirring time of 10 min promoted the formation of irregular cubic-like samples with visible defects on the surface. Control experiments imply that the stirring time of mixed $AgNO_3$ and ammonia plays a crucial role in the generation of

regular cubic Ag_3PO_4 microcrystals, which is closely related with the reactions between Ag_3PO_4, ammonia and Na_2HPO_4 [7,29].

The XRD patterns of as-synthesized cubic Ag_3PO_4 microcrystals are shown in Fig. 3a and all of the diffraction peaks can be identified to the body-centered cubic phase of Ag_3PO_4 (JCPDS No. 06-0505). It is well-known that Raman spectroscopy plays an important role in estimating the category of materials, thus Raman spectrum of Ag_3PO_4 was recorded and is shown in Fig. 3b. Several characteristic bands corresponding to the vibrations of Ag_3PO_4 appeared in the region below 1200 cm^{-1}, which can be assigned to different modes of Ag_3PO_4 sample including external modes, the bending vibration of the tetrahedral PO_4 ionic group, and the symmetric stretch of P–O–P and O–P–O bonds. It is believed that visible light absorption of the material is crucial in determining its photocatalytic performance, especially for the degradation and removal of organic pollutants under visible light irradiation. Thus diffuse reflectance spectra of irregular and cubic Ag_3PO_4 samples were recorded and are shown in Fig. 3c. It is notable that irregular Ag_3PO_4 shows good absorbance in the whole region, when the Ag_3PO_4 sample was obtained in a cubic form, an enhanced visible light absorption was observed, indicating that the generation of cubic Ag_3PO_4 favors better light absorption. Furthermore, a plot of the transformed Kubelka–Munk function of light energy $(\alpha hv)^2$ versus energy (hv) is also shown in Fig. 3d. According to the function, the band gaps of irregular and cubic Ag_3PO_4 samples were determined to be 2.42 eV and 2.38 eV, respectively.

Consequently the photocatalytic performance of the cubic Ag_3PO_4 microcrystals and irregular Ag_3PO_4 samples were evaluated using the degradation of organic dye molecules under visible-light irradiation as a model reaction, and the results are shown in Fig. 4. It is clearly shown from Fig. 4a that the photocatalytic efficiency of cubic Ag_3PO_4 microcrystals over RhB is higher than that of Ag_3PO_4 with irregular morphology, where the former sample is able to depose nearly all RhB molecules in 30 min and the latter merely achieve 80% degradation at the same time interval. Compared with irregular Ag_3PO_4 materials, the as-prepared cubic Ag_3PO_4 samples exhibited a higher photocatalytic activity over RhB. Furthermore, the photocatalytic performance of the cubic Ag_3PO_4 photocatalyst over different organic dyes RhB, MB and MO were also investigated. The results in Fig. 4b indicate that a higher photocatalytic degradation rate was achieved for RhB compared to MB and MO.

Moreover, reactive species trapping experiments of cubic Ag_3PO_4 photocatalyst over RhB were performed in order to investigate the reactive oxygen species in the photocatalytic process. Three chemicals, *p*-benzoquinone (denoted as BZQ, a $O_2^{-\bullet}$ radical scavenger), disodium ethylenediaminetetraacetate (Na_2-EDTA, a hole scavenger) and *tert*-butanol (a $\cdot OH$ radical scavenger) were employed. It is clearly shown in Fig. 4c that the introduction of *tert*-butanol into the photocatalytic system had no deleterious effect on the photocatalytic performance of cubic Ag_3PO_4 photocatalyst over organic dye RhB, whereas the addition of 5 mM BZQ into the photocatalytic system leads to the significant decrease in the photocatalytic degradation efficiency of RhB from almost 100% to around 20% in 40 min. Moreover, the introduction of 1 mM Na_2-EDTA into the same system caused fast deactivation of cubic Ag_3PO_4 photocatalyst with an efficiency less than 10% under visible light irradiation for 40 min. A possible explanation could lie in the EDTA anion absorption on the surface of cubic Ag_3PO_4 photocatalyst acting as a hole trap or electron donor. Since the nature of the photocatalytic process generally occurs on the surface of the photocatalyst, fast electron–hole recombination on the surface results in the deactivation of cubic Ag_3PO_4 photocatalyst. The addition of BZQ to the same photocatalytic system results in the significant capture of irradiated $O_2^{-\bullet}$ by BZQ and the obvious decrease in the amount of active $O_2^{-\bullet}$ radicals for photocatalytic reactions, suggesting an inefficient photocatalytic process. Furthermore, the fact that *tert*-butanol has no obvious effect on the photocatalytic activity of cubic Ag_3PO_4 photocatalyst implies that $O_2^{-\bullet}$ radicals and holes contribute majorly to its improved visible light photocatalytic performance while $\cdot OH$ radicals do not.

4. Conclusion

In conclusion, we have developed a facile deposition–precipitation method to fabricate cubic Ag_3PO_4 microcrystals. It is suggested that the addition of ammonia in the precursor effectively tailor the size and morphology of as-synthesized Ag_3PO_4 particles, and more importantly, the generation of cubic morphology can obviously improve the visible-light-driven photocatalytic degradation of Ag_3PO_4 over organic dye RhB. The results reveal that the cubic Ag_3PO_4 microcrystal is a promising candidate for the large-scale production of highly active visible-light driven photocatalytic materials.

Acknowledgments

This work was supported by the National Natural Science Foundation of China (51102116), Natural Science Foundation of Jiangsu Province of China (BK2011480). A Project Funded by the Priority Academic Program Development of Jiangsu Higher Education Institutions (PAPD), Natural Science Foundation of Jiangsu Higher Education Institutions of China (10KJB430001) and Scientific Research Foundation for Advanced Talents, Jiangsu University (10JDG057).

References

[1] Q.J. Xiang, J.G. Yu, M. Jaroniec, Graphene-based semiconductor photocatalysts, Chemical Society Reviews 41 (2012) 782–796.
[2] H. Tong, S.X. Ouyang, Y.P. Bi, N. Umezawa, M. Oshikiri, J.H. Ye, Nano-photocatalytic materials: possibilities and challenges, Advanced Materials 24 (2012) 229–251.
[3] A. Kubacka, M. Fernandez-Garcia, G. Colon, Advanced nanoarchitectures for solar photocatalytic applications, Chemical Reviews 112 (2012) 1555–1614.
[4] X.H. Guan, J.S. Du, X.G. Meng, Y.K. Sun, B. Sun, Q.H. Hu, Application of titanium dioxide in arsenic removal from water: a review, Journal of Hazardous Materials 215 (2012) 1–16.

[5] X.Q. An, J.C. Yu, Graphene-based photocatalytic composites, RSC Advances 1 (2011) 1426–1434.
[6] Z.G. Yi, J.H. Ye, N. Kikugawa, T. Kako, S.X. Ouyang, H. Stuart-Williams, H. Yang, J.Y. Cao, W.J. Luo, Z.S. Li, Y. Liu, R.L. Withers, An orthophosphate semiconductor with photooxidation properties under visible-light irradiation, Nature Materials 9 (2010) 559–564.
[7] Y. Bi, S. Ouyang, N. Umezawa, J. Cao, J. Ye, Facet effect of single-crystalline Ag_3PO_4 sub-microcrystals on photocatalytic properties, Journal of the American Chemical Society 133 (2011) 6490–6492.
[8] Q.H. Liang, W.J. Ma, Y. Shi, Z. Li, X.M. Yang, Hierarchical Ag_3PO_4 porous microcubes with enhanced photocatalytic properties synthesized with the assistance of trisodium citrate, CrystEngComm 14 (2012) 2966–2973.
[9] Y.P. Bi, H.Y. Hu, Z.B. Jiao, H.C. Yu, G.X. Lu, J.H. Ye, Two-dimensional dendritic Ag_3PO_4 nanostructures and their photocatalytic properties, Physical Chemistry Chemical Physics 14 (2012) 14486–14488.
[10] X.T. Hong, X.H. Wu, Q.Y. Zhang, M.F. Xiao, G.L. Yang, M.R. Qiu, G. C. Han, Hydroxyapatite supported Ag_3PO_4 nanoparticles with higher visible light photocatalytic activity, Applied Surface Science 258 (2012) 4801–4805.
[11] R.Y. Liu, P.G. Hu, S.W. Chen, Photocatalytic activity of Ag_3PO_4 nanoparticle/TiO_2 nanobelt heterostructures, Applied Surface Science 258 (2012) 9805–9809.
[12] Z.B. Jiao, Y. Zhang, H.C. Yu, G.X. Lu, J.H. Ye, Y.P. Bi, Concave trisoctahedral Ag_3PO_4 microcrystals with high-index facets and enhanced photocatalytic properties, Chemical Communications 49 (2013) 636–638.
[13] J. Wang, F. Teng, M.D. Chen, J.J. Xu, Y.Q. Song, X.L. Zhou, Facile synthesis of novel Ag_3PO_4 tetrapods and the {110} facets-dominated photocatalytic activity, CrystEngComm 15 (2013) 39–42.
[14] L.L. Zhang, H.C. Zhang, H. Huang, Y. Liu, Z.H. Kang, Ag_3PO_4/SnO_2 semiconductor nanocomposites with enhanced photocatalytic activity and stability, New Journal of Chemistry 36 (2012) 1541–1544.
[15] H.C. Zhang, H. Huang, H. Ming, H.T. Li, L.L. Zhang, Y. Liu, Z. H. Kang, Carbon quantum dots/Ag_3PO_4 complex photocatalysts with enhanced photocatalytic activity and stability under visible light, Journal of Materials Chemistry 22 (2012) 10501–10506.
[16] W.F. Yao, B. Zhang, C.P. Huang, C. Ma, X.L. Song, Q.J. Xu, Synthesis and characterization of high efficiency and stable Ag_3PO_4/TiO_2 visible light photocatalyst for the degradation of methylene blue and rhodamine B solutions, Journal of Materials Chemistry 22 (2012) 4050–4055.
[17] S.B. Rawal, S.D. Sung, W.I. Lee, Novel Ag_3PO_4/TiO_2 composites for efficient decomposition of gaseous 2-propanol under visible-light irradiation, Catalysis Communications 17 (2012) 131–135.
[18] Y.P. Liu, L. Fang, H.D. Lu, L.J. Liu, H. Wang, C.Z. Hu, Highly efficient and stable Ag/Ag_3PO_4 plasmonic photocatalyst in visible light, Catalysis Communications 17 (2012) 200–204.
[19] Y.P. Liu, L. Fang, H.D. Lu, Y.W. Li, C.Z. Hu, H.G. Yu, One-pot pyridine-assisted synthesis of visible-light-driven photocatalyst Ag/Ag_3PO_4, Applied Catalysis B: Environmental 115 (2012) 245–252.
[20] L. Liu, J.C. Liu, D.D. Sun, Graphene oxide enwrapped Ag_3PO_4 composite: towards a highly efficient and stable visible-light-induced photocatalyst for water purification, Catalysis Science and Technology 2 (2012) 2525–2532.
[21] Q.H. Liang, Y. Shi, W.J. Ma, Z. Li, X.M. Yang, Enhanced photocatalytic activity and structural stability by hybridizing Ag_3PO_4 nanospheres with graphene oxide sheets, Physical Chemistry Chemical Physics 14 (2012) 15657–15665.
[22] G.P. Li, L.Q. Mao, Magnetically separable Fe_3O_4–Ag_3PO_4 sub-micrometre composite: facile synthesis, high visible light-driven photocatalytic efficiency, and good recyclability, RSC Advances 2 (2012) 5108–5111.
[23] Y. Hou, F. Zuo, Q. Ma, C. Wang, L. Bartels, P.Y. Feng, Ag_3PO_4 oxygen evolution photocatalyst employing synergistic action of Ag/AgBr nanoparticles and graphene sheets, Journal of Physical Chemistry C 116 (2012) 20132–20139.
[24] J. Cao, B.D. Luo, H.L. Lin, B.Y. Xu, S.F. Chen, Visible light photocatalytic activity enhancement and mechanism of AgBr/Ag_3PO_4 hybrids for degradation of methyl orange, Journal of Hazardous Materials 217 (2012) 107–115.
[25] Y.P. Bi, H.Y. Hu, S.X. Ouyang, Z.B. Jiao, G.X. Lu, J.H. Ye, Selective growth of Ag_3PO_4 submicro-cubes on Ag nanowires to fabricate necklace-like heterostructures for photocatalytic applications, Journal of Materials Chemistry 22 (2012) 14847–14850.
[26] Y.P. Bi, H.Y. Hu, S.X. Ouyang, Z.B. Jiao, G.X. Lu, J.H. Ye, Selective growth of metallic ag nanocrystals on Ag_3PO_4 submicro-cubes for photocatalytic applications, Chemistry: A European Journal 18 (2012) 14272–14275.
[27] Y.P. Bi, S.X. Ouyang, J.Y. Cao, J.H. Ye, Facile synthesis of rhombic dodecahedral AgX/Ag_3PO_4 (X=Cl, Br, I) heterocrystals with enhanced photocatalytic properties and stabilities, Physical Chemistry Chemical Physics 13 (2011) 10071–10075.
[28] J.J. Buckley, A.F. Lee, L. Olivi, K. Wilson, Hydroxyapatite supported antibacterial Ag_3PO_4 nanoparticles, Journal of Materials Chemistry 20 (2010) 8056–8063.
[29] Y.P. Bi, H.Y. Hu, S.X. Ouyang, G.X. Lu, J.Y. Cao, J.H. Ye, Photocatalytic and photoelectric properties of cubic Ag_3PO_4 sub-microcrystals with sharp corners and edges, Chemical Communications 48 (2012) 3748–3750.